JONRA

Journal of Nuclear Research and Applications

Research Paper

Vol. 3, No. 4, P 40-46, Autumn (2023)

Cited in: https://jonra.nstri.ir

Received: 28 February 2023, Revised: 27 May 2023, Accepted: 24 June 2023

Molecular Dynamics Study of Microstructural Evolution and Damage-Depth Induced by Isotropic Irradiation on Zr-1%Nb Alloy

M. R. Basaadat*, S. Sheykhi

School of Physics & Accelerators, Nuclear Science and Technology Research Institute, (NSTRI), AEOI, P. O. Box 14395-836, Tehran, Iran.

ABSTRACT

Zirconium alloys with niobium have extensive applications in the nuclear industry, especially in fuel cladding. In this study, we consider the lattice structure of Zr-1%Nb alloy and study the damage depth (DD) due to irradiation on the structure of this alloy which results from the collision cascade (CC) phenomenon. It has been shown that the DD in the structure is directly related to Primary Knocked-on Atom (PKA) energy. Because the structure of Zr-1%Nb is not homogeneous, DD is highly affected by the incident direction of irradiation. Both Zr and Nb atoms were considered as PKA's and the results show that the average of DD is larger for Nb than Zr. Next, the CC phenomenon has been considered for this alloy, and microstructure evolution has been studied at low temperatures and low PKA energy. The results show the formation of some self-interstitials (SI's) during the CC phenomenon and no SI clusters are observed.

***Keywords*:** Zirconium-Niobium Alloy; Collision-Cascade Phenomenon; Damage Depth; Molecular Statics.

1. Introductions

Because of low neutron absorption cross-section and high resistance against corrosion, zirconium-niobium alloys are used as structural materials and fuel cladding in nuclear power reactors [1-4]. The study of microstructure evolution of the ZrNb alloy is, therefore, important when subjected to energetic irradiations due to fission in reactors. According to available data, there are three phases for crystalline zirconium: α-phase (< 863 ◦C), β-phase (> 863◦C), and ω-phase (Pressure 2-7 GPa) [5-7]. Zr-Nb alloys are limited to low Nb percentages (<5%). These alloys have a proper balance between corrosion resistance and low hydrogenation capacity [8]. In particular, Zr-1%Nb, which is studied in this work, has an HCP structure at low temperatures, and niobium atoms are dissolved in the Zr host structure. The structures of pure zirconium, niobium, and Zr-1%Nb alloy are shown

*. *Corresponding Author name*: M. R. Basaadat
E-mail address: mbasaadt@aeoi.org.ir

in Figure 1. Under irradiation, the atoms may displace irreversibly from their equilibrium lattice sites and give rise to the formation of defects. The resulting defects, then, may join together to make defect clusters. The macroscopic properties of nuclear materials are highly sensitive to the microstructural evolution of atoms in the materials and other parameters such as temperature and pressure. The present authors have already studied the mechanical properties of Zr-1%Nb alloy in the presence of defects [9, 10]. Also, other studies have been done by others [7-8,11-20] and some aspects of this alloy and other similar materials have been considered until now. But there are still a lot of open questions that researchers are working on.

This work is divided into three main steps: First, lattice structure properties have been calculated to verify the validity of the used interatomic potential in the calculations. Then, the damage depth (DD) value have calculated for Zr and Nb as PKA atoms, and the results of DD have compared. Finally, the CC phenomenon for low primary knocked-on atom (PKA) energies has been investigated.

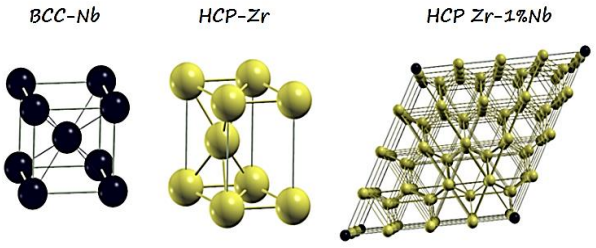

Fig. 1. Zirconium, Niobium, and Zr-1%Nb alloy structures at low temperatures.

2. Theories and Computational Details

All calculations have been done using atomistic simulation by the LAMMPS code package [21]. All post-processing has been done by VMD [22] visualizer and Gnuplot. Angular-dependent potential (ADP) is used as an interatomic potential for simulations. This new interatomic potential is used to simulate Zr-Nb alloy and can predict its mechanical properties correctly [23]. This kind of interatomic potential is commonly used for metals and metal alloys and it is a generalization of EAM[2] potential that includes dipole and quadrupole distortions of the local environment of an atom. The simulation box for studying Zr-1%Nb is an 8×8×7 supercell that contains 43008 atoms (with 96 atoms per unit cell) with dimensions of 103.4×89.6×108.1 $(^{\circ}A)^3$. This study has no temperature effect, so all calculations have been done at near zero (1 K) temperature. The structures have been fully optimized using the NPT ensemble and then the NVE ensemble has been used to simulate the CC phenomenon and DD processes. The 8 and 15 picoseconds were needed for equilibration of the structure in CC and DD phenomena when the structure has been subjected to radiation.

Table 1. Lattice constants in X & Z direction for pure-Zr (a,c) and Zr-1%Nb alloy in ˚A and VFE and SIFE for pure-Zr in eV. Reference data is composed of experimental and other available DFT calculations.

	Zr				Zr-1%Nb	
	a	***c***	***VFE***	***SIFE***	***a***	***c***
This work	3.188	5.206	1.9	2.76	12.856	15.360
Reference data	3.232[13]	5.149[13]	>1[24]	2.75[25]	-	-

3. Results and Discussion

3.1. Lattice Parameters

At first, the equilibrium lattice constants of pure-Zr in X and Z-directions (a,c) have been calculated and the results are in good agreement with experimental data. Because the structure of Zr-1%Nb is as pure-Zr, the calculations have been repeated to obtain the lattice constants of this alloy. Each unit cell of Zr-1%Nb has 96 atoms with an

2. Embedded Atom Method

HCP structure. The results have been listed in Table 1. Vacancy and self-interstitial formation energies (VFE, SIFE) are two important parameters when one is considering the defects in the structure. In other words, the value of VFE and SIFE can show the behavior of the structure, when it is involved in irradiation-induced defects. These quantities can be calculated as [7]:

$$E_V^f(p) = E(N-1;P) - \frac{N-1}{N}E(N;P) \quad (1)$$

$$E_{SI}^f(p) = E(N+1;P) - \frac{N+1}{N}E(N;P) \quad (2)$$

where $E_V^f(p)$, $E_{SI}^f(p)$ are VFE and SIFE in constant pressure respectively and N is the number of atoms in the structure. In addition, E(N ± 1; P), E(N; P) are the total energy with one excess/less atom and perfect system. Formation energies for pure Zr structure have also been listed in Table 1 and compared with experimental results. A pair of vacancy and self-interstitial is called Frenkel-pair (FP) and the formation energy of FP's (FPFE) is simply the sum of VFE and SIFE and for pure-Zr FPFE is 4.66 eV . According to these results, the used interatomic potential is reliable to simulate the CC phenomenon.

3. 2. Damage Depth

The damage depth (DD) is the maximum distance of the PKA position to the furthest SI, that is, the maximum length which is affected by the irradiation. On the other hand, this factor is a damage criterion of the structure for each incident energetic particle. The DD of Zr-1%Nb alloy directly shows the strength of this alloy when it is subjected to irradiation and it is highly dependent on the irradiation with respect to crystalline orientations. This spatial angle dependency is depicted in Figures 2 and 3 for different PKA energies. X and Y and Z axis in Fig 2 are θ, ϕ and DD respectively. The orientation space of irradiation has meshed for different polar and azimuthal angles. The polar and azimuthal angles are varied in the ranges of (0-90°) and (0-120°) and the mesh step is 15° for each angle. The energy of PKA atoms in Fig2a to 2e are 10, 50, 100, 200 and 300 eV respectively.

When this alloy is subjected to irradiation, PKA atoms can be Zr or Nb atoms. Therefore, the results of damage of the structure can be different for different PKA atom types. In general (Fig2a to 2e), DD is bigger for Nb-PKA atoms in this structure. Therefore, the damage range for Nb as PKA atoms is more than Zr.

For E(PKA) = 10 eV, DD values are zero for nearly all directions. From experimental data, [26] the threshold displacement energy for Zirconium structure to produce a stable FP is about 22.5 eV. According to our calculation for PKA energy between 20-30 eV stable FP can be seen in most directions.

The left side of Figure 3 is related to Zr-PKA atoms and the right side to Nb. From this figure, it is clear that DD for E(PKA) = 50 eV for Zr and Nb-PKA are nearly the same and are changing (0-40) ˚A. DD for E(PKA) = 100, 200, and 300 eV for Nb-PKA is meaningfully more than Zr-PKA, and for 100 eV is in the range of (11-37), (11-45) ˚A. This factor for 200 eV PKA energy is about (16-62), (24-84). Finally, for 300 eV PKA energy, DD is changed as (19-73) and (34-90) ˚A for Zr- and Nb-PKA atoms. It is shown that the maximum DD is happened for a head-on collision with nearest neighbor atoms such as X-direction (θ = 90 & ϕ = 0), as can be seen in Figure 3.

Furthermore, there are 8 SI positions in Zr-1%Nb which show in Figure 4 and the results show that for E(PKA) = 300 eV , the maximum of DD can be nearly seen in the direction of the octahedral SI position (θ = 55.4 & ϕ = 30). In other words, when the direction of irradiation is in the SI direction of the structure, the furthest atoms can be placed in the SI positions after losing their energy during the CC process.

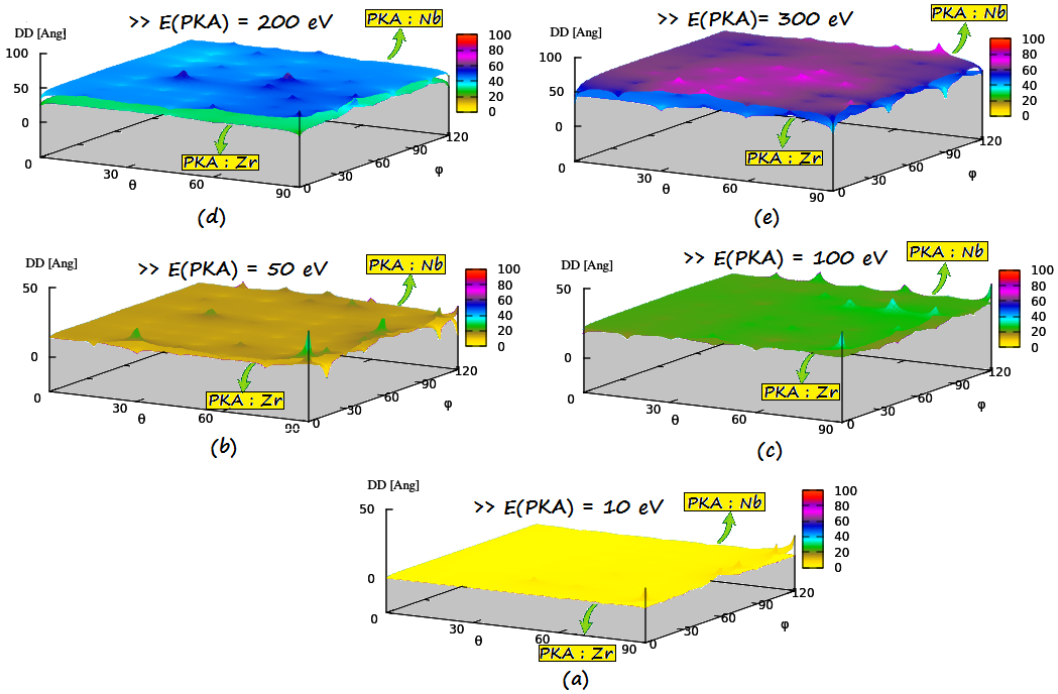

Fig. 2. The dependency of DD to the polar and azimuthal angles of irradiation for different E(PKA): **a.** E(PKA) = 10 eV, **b.** E(PKA) = 50 eV, **c.** E(PKA) = 100 eV, **d.** E(PKA) = 200 eV, **e.** E(PKA) = 300 eV.

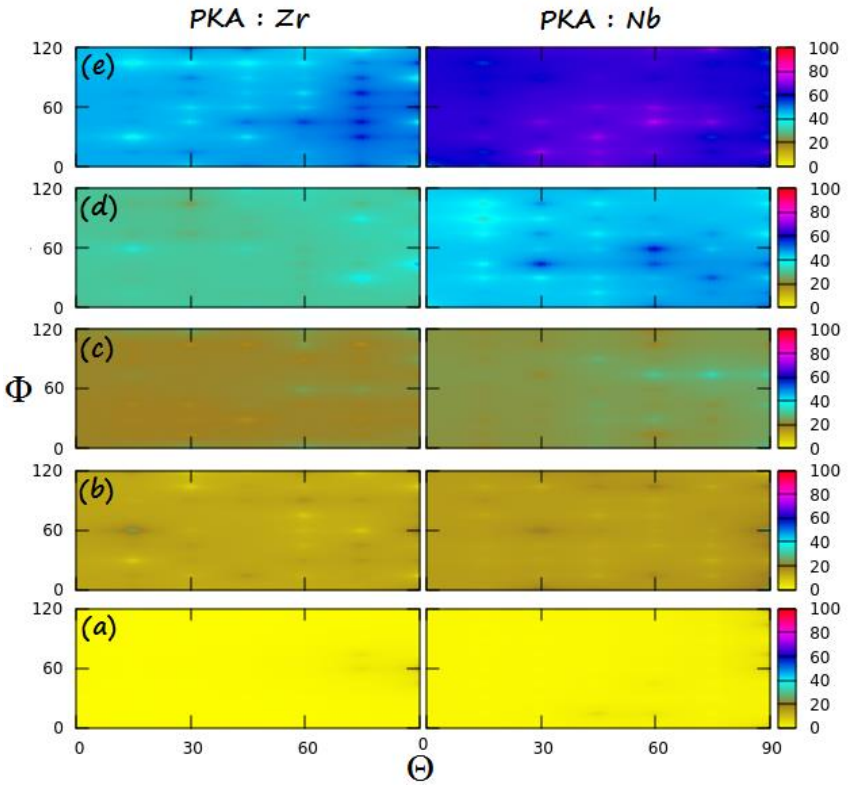

Fig. 3. The 2D map dependency of DD to the polar and azimuthal angles of irradiation for different E(PKA): **a.** E(PKA) = 10 eV, **b.** E(PKA) = 50 eV, **c.** E(PKA) = 100 eV, **d.** E(PKA) = 200 eV, **e.** E(PKA) = 300 eV.
The first (V) and second vacancy positions (N1 to N5) in the HCP zirconium structure; N1 to N5 refer to 1st to 5th nearest neighbor structure positions.

Table 2. The average DD for different E(PKA) in ˚A and eV respectively.

E(PKA)	10	50	100	200	300
AVGDD; Zr-PKA	0.8	13.7	21.4	31.5	47.2
AVGDD; Nb-PKA	1.7	16.0	24.1	45.2	63.2

It has also been shown that an increase in the E(PKA) can lead to an increase in DD. Furthermore, the treatment of the mean value of all DD in these orientations with respect to the PKA energy has a deviation from linear relation and is shown in Table 2 and Figure 5. In other words, the DD variation with respect to E(PKA) is similar to the NRT model. When the PKA energy for this alloy is near 300 eV, it means that the order of irradiation energy is about a few hundred eV. Hence, when the Zr-1%Nb structure is subjected to irradiation with relatively high energy the structure is affected nearly by 40 ~ 60 ˚A.

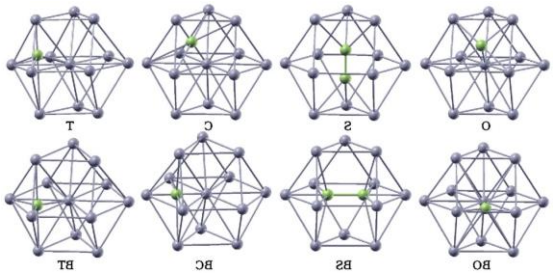

Fig. 4. Eight SI positions in Zr-1%Nb alloy; O: octahedral, S: split-dumbble, C: crowdion, T: tetrahedral and B in 4 bottom stand for basal [7].

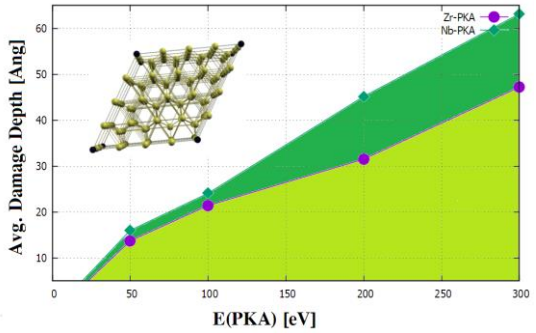

Fig. 5. DD variation w.r.t. E(PKA) for Zr-1%Nb alloy.

3. 3. Collision Cascade (CC) Phenomenon

CC phenomenon has been considered for Zr-1%Nb alloy in this section. This phenomenon is illustrated in Figure 6. When PKA atoms have sufficient kinetic energy to transfer to the atoms nearby the PKA atoms, they are displaced from their equilibrium crystal lattice sites, leaving behind a vacant site or a vacancy and each displaced atom and its vacancy make an FP. The FPs, themselves, may have acquired sufficient energy to displace other atoms and this process can be repeated to make the CC phenomenon. At first, the number of FPs increases, then some of the displaced atoms recombine with vacant sites and the number of FPs decreases over time. So all of the available FPs are not stable and just a few FPs will remain in the structure. For Zr-1%Nb alloy, the most disturbed structure takes place around 0.5 picoseconds and the equilibration is achieved after 15 picoseconds. As it can be seen, no clustering of defects has been detected individually for low PKA energies and temperature in a perfect crystal. It is clear that for high PKA energies it is possible to find clusters of Self-Interstitials (SIs) or voids (V).

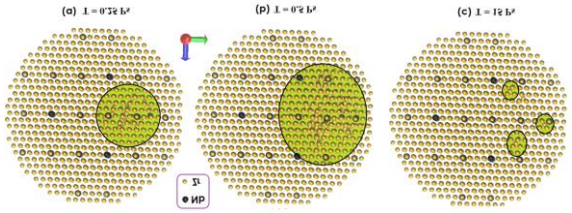

Fig. 6. CC phenomenon for Zr-1%Nb alloy for different time steps.

4. Conclusion

In this study, the DD of the PKA atoms with different energies for Zr-1%Nb alloy has been calculated and the results have shown that the increase in PKA energy can lead to an increase in DD. In addition, the Nb and Zr atoms may be taken as PKA atoms and the change in the type of PKA atoms changes the damage depth of the alloy. It has been shown that Nb-PKA atoms can produce more

damage to the structure. Furthermore, DD was meaningfully dependent on irradiation orientation and this dependency has been explored in homogeneous angle meshes and it has been shown that in some cases, the direction of SI in HCP structure may lead to higher degrees of damage. The CC phenomenon was also considered for this alloy and it has been shown that a few Frenkel pairs were produced in low PKA energies.

5. Abbreviations

The following abbreviations are used in this manuscript:

DD	Damage Depth
CC	Collision Cascade
PKA	Primary Knocked-on Atom
SI	Self-Interstitial
HCP	Hexagonal Close-packed
BCC	Body-Centered cubic
ADP	Angular Dependent Potential
EAM	Embedded Atom Method
DFT	Density Functional Theory
VFE	Vacancy Formation Energy
SIFE	Self-Interstitial Formation Energy
FP	Frenkel Pair
FPFE	Frenkel Pair Formation Energy
NRT	Norgett, Robinson, and Torres

References

1. Bell BDC, Murphy ST, Burr PA, Comstock RJ, Partezana JM, Grimes RW and Wenman MR. The influence of alloying elements on the corrosion of Zr alloys. Corrosion Science 105 PP. 36–43, 2016.
2. Fernandez G, et. al. Zeitschrift f¨ur Metallkunde 82 (6) PP. 478–487, 1991.
3. Lustman B, Kerze F. The metallurgy of zirconium. (McGraw-Hill Book Company 1955 4).
4. Cox B. Some thoughts on the mechanisms of in-reactor corrosion of zirconium alloys. Journal of Nuclear Materials. 336 (2) P 331–368, 2005.
5. Xia H, Duclos S J, Ruoff A L, Vohra Y K. New high-pressure phase transition in zirconium. Metal Phys. Rev. Lett. 64 (2), 1990.
6. Kharchenko V O, Kharchenko D O. Ab-initio calculations for structural properties of Zr-Nb alloys. arXiv preprint arXiv. 1206.7035, 2012.
7. Peng Q, Ji W, Lian J, Chen X J, Huang H, Gao F and De S. Pressure effect on stabilities of self-Interstitials in HCP-Zirconium Scientific reports, Nature Publishing Group. 41 (1), P 1-7, 2014.
8. D Smirnova, S Starikov. Defect and Diffusion Forum. Study of niobium diffusion and clusterization in hcp zr-nb dilute alloys. Trans Tech Publ. 375, P 167–174, 2017.
9. Basaadat M R, Payami M. Elastic stiffness tensors of Zr–Nb alloy in the presence of defects: A molecular dynamics study. International Journal of Modern Physics. C 31 (02), P 2050028, 2020.
10. Basaadat M R, Payami M. The study of the properties of point defects in pure-Zr and Zr-1% Nb alloy using density-functional theory and atomic simulation. Iranian Journal of Physics Research. 20 (1), P 57–64, 2020.
11. Xin X K, Lai W S, Liu B X. Point defect properties in hcp and bcc Zr with trace solute Nb revealed by ab initio calculations. Journal of Nuclear Materials. 393 (1), P 197–202, 2009.
12. Wang X, Liu L B, Wang M F, Shi X, Huang G X, Zhang L G. Computational modeling of elastic constants as a function of temperature and composition in Zr–Nb alloys. Calphad 48 (1), P 89–94, 2015.
13. Fisher ES, Renken CJ. Single-crystal elastic moduli and the hcp→ bcc transformation in Ti, Zr, and Hf. Physical review 135 (2A), P A482, 1964.

14. Ashkenazi J, Dacorogna M, Peter M, Talmor Y, Walker E, Steinemann S. Elastic constants in Nb-Zr alloys from zero temperature to the melting point: Experiment and theory. Physical Review B 18 (8), P 4120, 1978.

15. Bolef DI. Elastic constants of single crystals of the bcc transition elements V, Nb, and Ta. Journal of Applied Physics 32 (1), P 100–105, 1961.

16. Weck P F, Kim E, Tikare V, Mitchell J A. Mechanical properties of zirconium alloys and zirconium hydrides predicted from density functional perturbation theory. Dalton Transactions, 44 (43), P 18769–18779, 2015.

17. Hayes DJ, Brotzen FR. Elastic constants of niobium-rich zirconium alloys between 4.2 K and room temperature. Journal of Applied Physics. 45 (4), P 1721–1725, 1974.

18. Varshni YP. Temperature dependence of the elastic constants. Physical Review B 2 (10), P 3952, 1970.

19. Fast L, Wills JM, Johansson B, Eriksson O. Elastic constants of hexagonal transition metals: Theory Physical Review. B 51 (24), P 17431, 1995.

20. Al-Zoubi N, Ch¨onecker S, Li X, Li W, Johansson B, Vitos L. Elastic properties of 4d transition metal alloys: Values and trends. Computational materials science. 159, P 273–280, 2019.

21. Plimpton S J LAMMPS features and capabilities. Sandia National Lab. (SNL-NM), Albuquerque, NM (United States) 2014.

22. Humphrey W, Dalke A, Schulten K. VMD - Visual Molecular Dynamics, J. Molec. Graphics, vol. 14, pp. 33-38, 1996.

23. Smirnova DE, Starikov SV. An interatomic potential for simulation of Zr-Nb system. Computational Materials Science. 129, P 259–272, 2017.

24. Swanson ML, Piercy GR, Kidson GV. Quenneville AF, Atomic Energy of Canada Ltd., Chalk River (Ontario). Chalk River Nuclear Labs 1969.

25. Samolyuk G D, Golubov S I, Osetsky YN, Stoller R E. Self-interstitial configurations in hcp Zr: a first principles analysis. Philosophical magazine letters. 93 (2), P 93–100, 2013.

26. WG Wolfer, Comprehensive nuclear materials 1, P 1–45, 2012.

How to cite this article

M. R. Basaadat, S. Sheykhi, *Molecular Dynamics Study of Microstructural Evolution and Damage-Depth Induced by Isotropic Irradiation on Zr-1%Nb Alloy*, Journal of Nuclear Science and Applications (JONRA), Vol. **3,** No. **4,** P **40-46,** Autumn **(2023),**

Url: https://jonra.nstri.ir/article_1581.html**, DOI**: https://doi.org/10.24200/jon.2023.1074.